04,08,16

Dielectric-spectroscopic separation of characteristics of conduction mechanisms in AgI nanocrystalline films

© A.V. Ilyinsky[1], R.A. Kastro[2], A.A. Kononov[2], M.E. Pashkevich[3], E.B. Shadrin[1,¶]

[1] Ioffe Institute,
St. Petersburg, Russia
[2] Herzen State Pedagogical University of Russia,
St. Petersburg, Russia
[3] Peter the Great Russian State Polytechnic University,
St. Petersburg, Russia

¶ E-mail: shadr.solid@mail.ioffe.ru

Received June 13, 2023
Revised June 13, 2023
Accepted June 27, 2023

The study of the frequency dependence of the components of the complex permittivity of thin (100 nm) nanocrystal silver iodide (AgI) films revealed the presence of two different types of relaxation processes, sharply differing in their relaxation times: $\tau_1 \ll \tau_2$. It is established that the small relaxation time of τ_1 is the time of formation of a stable configuration of the internal electric field when the external high-frequency sinusoidal electric field is shielded by a system of free conduction electrons. On the contrary, a long relaxation time of τ_2 characterizes the process of shielding a low-frequency external field by a system of quasi-free silver ions. It is shown that the temperature dependence of the numerical value of $\tau_1(T)$ has a thermal hysteresis with a loop, the position of the heating and cooling branches of which coincides with the temperature region of the forward and reverse phase transitions in the AgI film: semiconductor-superionic and superionic-semi-conductor. The results of calculating the parameters of dielectric spectra in the framework of Debye theory are presented, demonstrating good agreement with the parameters of the proposed electrical circuit of the film sample calculated by the complex impedance method

Keywords: dielectric measurements, superionics, silver iodide, semiconductor-superionic phase transition.

DOI: 10.61011/PSS.2023.08.56571.109

1. Introduction

The relevance of obtaining detailed information about the electrical properties of superionics is determined not only by the demand for the use of film materials created on the basis of superionics in a wide range of applied devices, but also by the lack of information about methods for controlling the physical parameters of processes occurring in superionics. The latter is due to the lack of detailed information about the superionic phase transitions (PT) occurring in these materials.

This gap can be filled by applying the dielectric method of measuring the characteristics of thin nanocrystalline films of superionics, which, as experience shows, proved to be very informative due to the use of highly sensitive industrial dielectric spectrometers with modern computer equipment in the research process. This paper studies dielectric spectra (DS) of thin films of a superionic such as silver iodide, in which two thermal PT are performed: a semiconductor–a semiconductor at a temperature of $T_c = 384\,\mathrm{K}$ (111°C) and a semiconductor–a superionic at a temperature of $T_c = 420\,\mathrm{K}$ (147°C).

It is known [1] that AgI exists in three different crystal modifications: γ, β and α-phases. A thermal superionic PT occurs at $T_c = 147$°C: β-the phase turns into a stable α-phase at 147°C. This phase has also ionic conductivity along with electronic being a superionic phase at $T > T_c$. β-phase has a lattice of hexagonal symmetry, α-phase has a volume-centered cubic lattice.

The DS investigated in this work represent the frequency dependences of the real $\varepsilon'(f)$ and imaginary $\varepsilon''(f)$ parts of the complex permittivity of the material $\varepsilon^* = \varepsilon' + i\varepsilon''$ in the low (20 Hz−1 MHz) and ultra-low (0.1 Hz−10 Hz) frequencies [2]. The dielectric loss angle tangent frequency dependences $\mathrm{tg}\,\delta(f) = \varepsilon''/\varepsilon'$ and Cole−Cole diagrams $\varepsilon''(\varepsilon')$ obtained based on this dependences are also positioned in the scientific literature as DS. The significance of the experimental determination of the parameters of the response of a material to the influence of an external alternating electric field of various frequencies obtained during DS measurements is determined by the fact that their numerical values carry fundamental information about the electrical properties of the material under study.

The purpose of this article was to study the features of the electrical response of a set of nanocrystalline grains of silver iodide synthesized on a mica substrate and forming an almost single-layer thin-film structure. Such characteristics of the electric response of AgI films as the frequency dependences of the complex permittivity $\varepsilon^*(f)$ and, in addition, the Cole−Cole diagrams of film samples

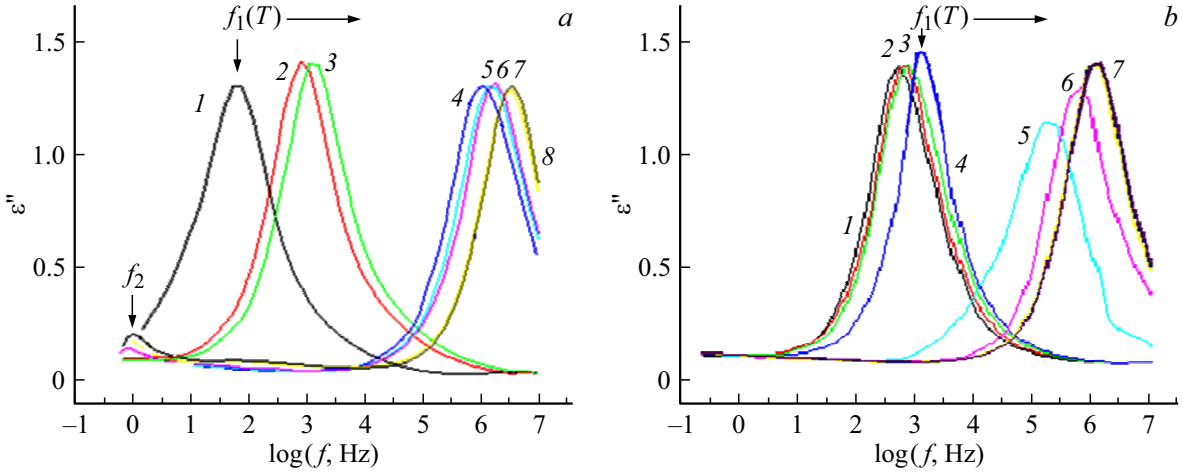

Figure 1. Frequency dependences of the imaginary part ε'' of the dielectric constant of the AgI film in the temperature range *a* — 70–250°C (*1* — 70, *2* — 130, *3* — 140, *4* — 150, *5* — 160, *6* — 170, *7* — 240, *8* — 250°C); *b* – 140–160°C (*1* — 140, *2* — 143, *3* — 146, *4* — 149, *5* — 152, *6* — 155, *7* — 158, *8* — 161°C).

(CC-diagrams) were studied. The studies carried out made it possible to determine the electrical characteristics of AgI films (type of conductivity, relaxation times of the dielectric response) before, during and after the thermal PT semiconductor-superionic in them. An equivalent electrical circuit of an AgI film sample is proposed, the parameters of the proposed equivalent electrical circuit are determined by the method of calculating the multiplex impedance, the calculated data are compared with the data of the DS experiment, and on this basis a conclusion is made about the validity of using the proposed equivalent circuit.

2. Experiment procedure

AgJ samples were thin (~ 100 nm) nanocrystalline films synthesized on mica substrates. The first stage of synthesis consisted in applying a thin (80 nm) layer of silver to a high-quality (optical) mica with a thickness of 40 μm by evaporation in vacuum, after which the mica heated to 150°C was placed 45 min into the atmosphere of iodine vapor. The vapors were created by the sublimation of crystalline iodine at a temperature of 110°C. An almost monolayer nanocrystalline film AgI was synthesized on mica in the result of the chemical interaction of iodine with silver.

Dielectric measurements were performed on a Novocontrol Technologies spectrometer. The spectrometer cell was a capacitor with electrodes made of two flat gilded plates with a diameter of 15 mm, between which the test sample with a thickness of $d \sim 40\,\mu$m was placed. The capacity of the C_0 empty cell was determined by the expression $C_0 = \varepsilon_0 S/d$. DS were measured in the frequency range 10^{-1}–10^7 Hz. The temperature of the T sample changed monotonically in the interval 70–240°C, and dielectric measurements were performed at fixed points with a step of 10°C. In the region of the superionic PT in AgI, namely, in the interval 140–160°C, the step in order to obtain additional details was reduced to 3°C. The frequency dependences of the real $\varepsilon'(f)$ and imaginary $\varepsilon''(f)$ parts of the complex permittivity were recorded as DS. For clarity of presentation and convenience of analysis of measurement results, the dependencies $\varepsilon'(f)$ and $\varepsilon''(f)$ were rearranged in the form of Col–Cole diagrams. Namely, in the form of dependencies $\varepsilon''(\varepsilon')$.

3. Experimental results

Fig. 1, *a* shows the frequency dependences of the imaginary $\varepsilon''(f)$ part of the permittivity of a silver iodide film sample. Maximum of the functional dependence $\varepsilon''(f)$ is located at the frequency $f_{\max 1} = 32$ Hz at $T = 70$°C. Maximum value of the function $\varepsilon''(f)$ is $\varepsilon''(f_{\max 1}) = 1.25$. The frequency at which the maximum of the function $\varepsilon''(f)$ is located monotonically increases from 32 Hz to 0.91 kHz with an increase of temperature in the range (70–140)°C and the numerical value of its magnitude practically does not change with frequency changes. The maximum shifts abruptly towards high frequencies in temperature range 140–600°C (curves *3, 4* Fig. 1, *a*) and is located already at 1 MHz at 160°C. Due to the smallness of the temperature interval of the abrupt increase in the frequency of the maximum, Fig. 1, *b* shows the results of a more detailed study of the thermal variation of the frequency dependencies $\varepsilon''(f)$ in the temperature range 140–160°C: the temperature here changed in increments of 3°C, which made it possible to more accurately determine the frequency positions $f_{\max 1}$ of the maximum function $\varepsilon''(f)$ at different temperatures, both during heating and cooling of the film sample. In addition, it turned out that an additional weakly pronounced maximum $\varepsilon''(f)$ occurs in the low-frequency region of the DS at higher temperatures ($T > 170$°C) (curves *7, 8* in Fig. 1, *a*). The numerical value of the function $\varepsilon''(f)$ in the second additional maximum is small: $\varepsilon''(f_{\max 2} = 0.2$,

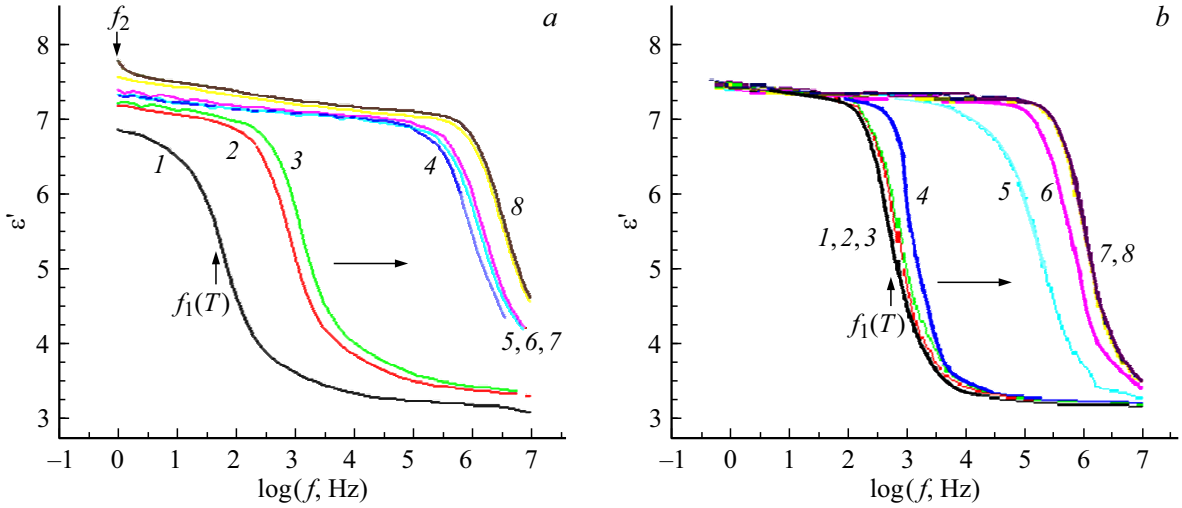

Figure 2. Frequency dependences of the real part ε' of the dielectric constant of the AgI film in the temperature range. *a* — 70–250°C (*1* — 70, *2* — 130, *3* — 140, *4* — 150, *5* — 160, *6* — 170, *7* — 240, *8* — 250°C); *b* — 140–160°C (*1* — 140, *2* — 143, *3* — 146, *4* — 149, *5* — 152, *6* — 155, *7* — 158, *8* — 161°C).

$f_{\max 2} = 1$ Hz. It is necessary to point out that the frequency maxima stabilized at $T > 160$°C, i.e. their displacement stopped.

Fig. 2, *a* shows the frequency dependences of the real part $\varepsilon'(f)$ of the complex permittivity. One step on this dependence with its middle part at the frequency $f_1 = 32$ Hz is observed at $T = 70$°C. It shifts towards high frequencies with an increase of temperature synchronously with the thermal shift of the maximum of the function $\varepsilon''(f)$. A weak additional step appears in the low-frequency region of the spectrum ($f_2 = 1$ Hz) at $T > 170$°C. The frequency position of the first (main) step of the function $\varepsilon'(f)$, as well as the position of the first maximum of the function $\varepsilon''(f)$, increases abruptly with an increase of temperature in the range from 140°C to 160°C: from 0.89 kHz to 1 MHz for functions $\varepsilon'(f)$, from 0.91 kHz to 1 MHz for the function $\varepsilon''(f)$. The parameters of the function $\varepsilon'(f)$ in this temperature range are measured in more detail — when the temperature changes in increments of 3°C (Fig. 2, *b*). When the temperature decreases, the DS features shown in Fig. 1, 2 return to their original position on the frequency scale, but with a temperature delay of 12°C.

Figure 3 shows the Cole–Cole diagrams $\varepsilon''(\varepsilon')$. They comprise semicircles, the appearance of which weakly depends on temperature in the entire temperature range, with the exception of the high temperature region: at $T > 160$°C, a part of an additional second semicircle of small radius appears in the right part of Fig. 3, which corresponds to low frequencies.

A careful measurement of the DS in the temperature range 140–160°C detects small changes in this interval of the form of the main semicircle. It has an irregular shape (compared to the ideal shape of the „Debye“ semicircle — the dotted curve in Fig. 3), and its center is located below the abscissa axis by 9% of the radius length. But at $T = 152$°C, the main semicircle again has an almost correct shape, although its center ($\Delta\varepsilon'' = 0.5$) drops another 20% below the radius length.

Thus, the following features of DS are observed in the experiment:

– a sharp shift in the frequency position of the high-frequency maximum of the function $\varepsilon''(f)$ and the frequency position of the main step of the function $\varepsilon'(f)$ in the interval $T = 140$–160°C;

– the appearance of an additional second maximum of the function $\varepsilon''(f)$ and an additional second step of the function $\varepsilon'(f)$ at low frequencies (curves *8*) at temperatures above 140°C;

– occurrence of a second additional semicircle on Cole-Cole diagrams at high temperatures.

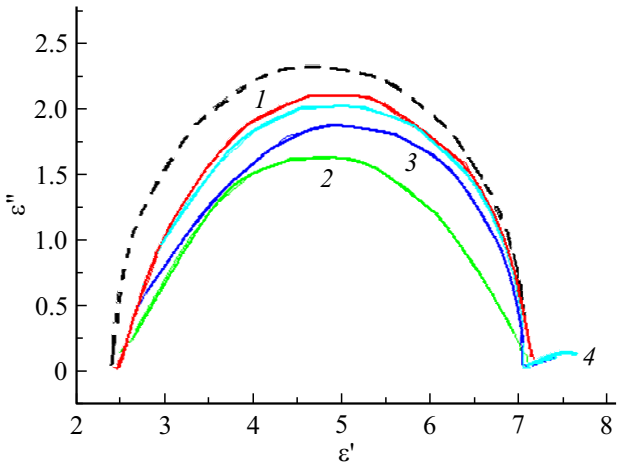

Figure 3. Cole–Cole diagrams of the AgI film for temperatures in the PT region (*1* — 149, *2* — 152, *3* — 155, *4* — 158°C). Dotted curve — „Debye“ semicircle with radius of 2.25.

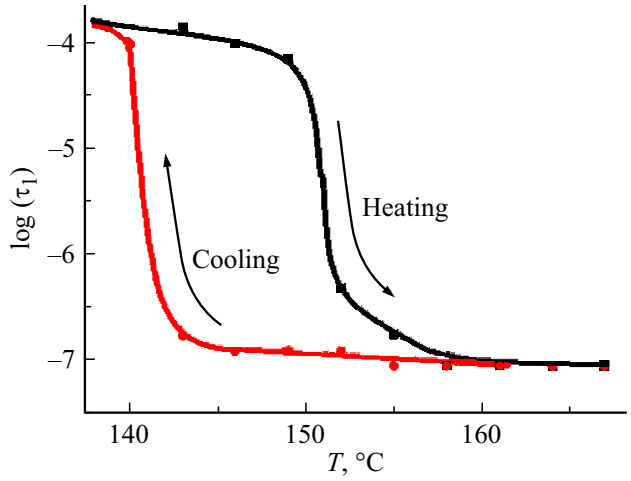

Figure 4. Temperature hysteresis loop $\mathrm{Log}(\tau_1)$, where $\tau_1 = 1/(2\pi f_1)$ is determined by the position of the maximum 1 imaginary part of $\varepsilon'(f)$ of the dielectric constant.

Looking ahead, we note that the above features of the DS indicate that in AgJ films at $T \sim 140°\mathrm{C}$, a semiconductor-superionic is performed. For this reason, two groups of relaxation time values $\tau_1 = 1/(2\pi f_1)$, determined by the frequency position $f_{\max 1}(T)$ of the maximum function $\varepsilon''(f)$ are shown in Fig. 4 for interval 140–160°C. One group corresponds to heating, the other — cooling of the AgI film sample. The figure shows that the curves smoothing out the spread of numerical values of the relaxation time at sequentially located temperature points form a characteristic loop — a loop of thermal hysteresis, the geometric center of which, located at half the span of the loop on a vertical scale, falls on the temperature $T_c = 147°\mathrm{C}$, i.e., the equilibrium temperature of the semiconductor and superionic phases.

4. Calculation results

Calculations of the frequency dependences of the components of the complex permittivity of the film based on the Debye theory [3] are performed in this paper to construct an adequate model of the electrical response of an AgI nanocrystalline film to the impact of low frequency external alternating electric field.

The DS was calculated for two types of relaxators with characteristic times τ_1 and τ_2, which, according to theory allows writing the complex permittivity ε^* in the form

$$\varepsilon^*(\omega) = \varepsilon_\infty + \frac{\Delta\varepsilon_1}{1 + (i\omega\tau_1)} + \frac{\Delta\varepsilon_2}{1 + (i\omega\tau_2)}, \qquad (1)$$

where ε_∞ — the high-frequency limit of the real part of the dielectric constant ε^*, $\Delta\varepsilon_1$ and $\Delta\varepsilon_2$ — the heights of the steps of the real part ε^*, $\omega = 2\pi f$ — angular frequency.

It is assumed for the calculations in this model that the distribution of relaxers by relaxation times within each type of relaxers is a delta function, i.e. each type of relaxers is characterized by a single relaxation time.

Figure 5 shows, on a logarithmic scale, graphs of the functions $\varepsilon'(f)$ and $\varepsilon''(f)$, constructed according to the formula (1), as well as the corresponding Cole-Cole diagram. Figure 5 shows that the functional dependence $\varepsilon''(f)$ has two maxima at frequencies $f_{\max 1}$ and $f_{\max 2}$, the dependence $\varepsilon'(f)$ has two steps at the same frequencies. The CC diagram $\varepsilon''(\varepsilon')$ has two regular semicircles of different diameters. Formula parameters (1) are selected in such a way that the calculated curves constructed correspond to the experimental curves obtained at a temperature of 250°C, i.e. at the temperature at which high-frequency and low-frequency DS features are simultaneously observed in the experiment. A comparison of the charts of these functions calculated using the formula (1) (Fig. 5) with the experimental charts presented in Fig. 1–3 shows that Debye theory qualitatively explains the type of DS films of silver iodide.

Note that all the values (ε_∞, $\Delta\varepsilon_1$, $\Delta\varepsilon_2$, $\tau_1 = 1/(2\pi f_1)$ and $\tau_2 = 1/(2\pi f_2)$) included in the formula (1), are determined from the experimental charts of Fig. 1–3. Therefore, the fact that the calculated curves coincide with the measured curves is not informative enough. Additional information about the mechanisms of physical processes that determine the type of DS can be obtained by using an equivalent electrical circuit adequate to the experimental conditions. Figure 6 shows a possible, in our opinion, equivalent scheme. The results of calculations performed on the basis of this scheme are shown in Fig. 7. The values

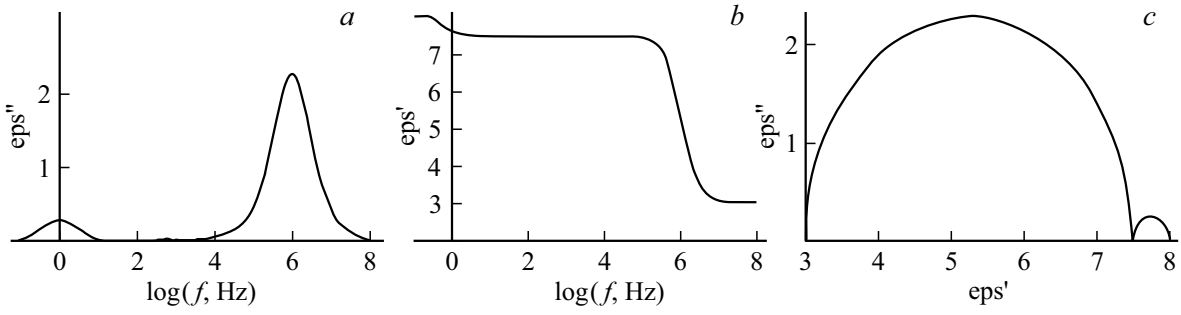

Figure 5. The frequency dependencies calculated using the formula (1) (*a*) imaginary ε'' and (*b*) valid ε' parts of the dielectric constant, (*c*) CC-diagram — dependence $\varepsilon''(\varepsilon')$.

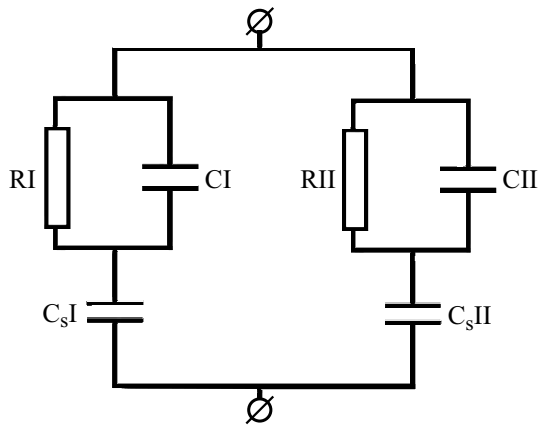

Figure 6. Equivalent scheme. C_sI, C_sII — capacities of parts of the dielectric (mica) substrate on which the AgI semiconductor film is synthesized, CI, CII — capacities of parts of the film, RI, RII — film resistances at electron and ionic conductivity, respectively.

of the scheme parameters are given in the figure caption. The calculation method is given in [4]. A comparison of the charts of the above functions (Fig. 7) obtained during the calculation based on the equivalent scheme of Fig. 6 shows that the equivalent scheme also satisfactorily explains the type of DS presented in Fig. 1–3.

5. Discussion of results

We believe that in our case, the values of the DS parameters (the frequency position of the steps $\varepsilon'(f)$, the maxima $\varepsilon''(f)$, the shape and position of the centers of the semicircles on the CC diagrams) are due to a specific type of relaxers. Namely, the high-frequency features are due to the relaxation time of the array of free electrons, and the low-frequency ones are due to the array of positively charged free silver ions. The characteristic relaxation time in this case is the Maxwell relaxation times $\tau_M = \varepsilon\varepsilon_0/\sigma$ [5], where σ — the specific electrical conductivity of the crystalline substance.

In a semiconductor film placed in a measuring cell mounted in the form of a flat capacitor, to which an external electric field of constant polarity is applied, free electrons are transferred in the direction of the positive electrode. In the case of a negative blocking electrode (mica substrate), the result of blocking is the predominance of the rate of thermal generation of electrons over the rate of their capture on traps. Therefore, a positive volumetric charge accumulates here. The accumulation time of a volume charge with a density of ρ and the rate of its shielding of the external field is determined by the Maxwell time: $\tau_M = \varepsilon\varepsilon_0/\sigma = \varepsilon\varepsilon_0/(\mathrm{e}\mu\mathrm{n})$, where e, μ, n — charge, drift mobility and concentration of free electrons, respectively. In the stationary case ($f = 0$), the thickness of the bulk charge layer is determined by the Schottky formula: $w = (2\varepsilon\varepsilon_0 U_{\mathrm{sem}}/\rho)^{1/2}$. The voltage applied to the dielectric cell V is distributed between the mica substrate bearing the AgI film (the voltage drop on the mica is U_s) and the semiconductor film (the voltage drop on the AgI film is U_{sem}): $V = U_s + U_{\mathrm{sem}}$. In other words, inside the semiconductor film, when the external field is shielded by an array of free electrons, this field is partially displaced into the dielectric substrate, but in the region of the volume charge, the field does not turn out to be zero (:div$\bar{E} = \rho/(\varepsilon\varepsilon_0)$ — Poisson equation). Since the total capacitance of the measuring dielectric cell is determined by two series-connected capacitors: $C_{\mathrm{total}} = C_s C_{\mathrm{sem}}/(C_s + C_{\mathrm{sem}})$, then when the external field is almost completely shielded by a semiconductor layer ($C_{\mathrm{sem}} \to \infty$), $C_{\mathrm{total}} \to C_s$ takes place. It follows that the real part of the complex permittivity of the cell is determined by the properties of the blocking mica substrate: $\varepsilon' \to C_s/C_0$. Nevertheless, the experiment shows that $\varepsilon' < C_s/C_0$, i.e. at zero frequency of external field oscillations ($f = 0$), there is no complete shielding of the external electric field (see, for example, the curves *1* in Fig. 2, 3).

When an alternating voltage is applied to the cell (at $T < T_c$), a volumetric positive charge accumulates in the semiconductor film from the side of the negative electrode alternately from one or the other side of the film. When an external voltage of low frequency is applied, the field shielding is, as indicated above, incomplete. When applying a high frequency voltage ($f \to \infty$), the maximum achievable in a dielectric spectrometer (10^7 Hz), there is practically no drift of free electrons due to the presence of low electron mobility in AgI, due to the high concentration of electron traps [6]. At the same time, the volumetric charge practically does not accumulate, and due to this, there is no shielding of the external field. In this case, the experiment detects the value of $\varepsilon' = C_s/C_0 = 2.5$, which implies that the semiconductor layer has an electrical capacity of $C_{\mathrm{sem}} = 3.6C_0$.

As the temperature increases, the rate of thermal electron generation increases, the thickness of the bulk charge layer decreases, and the Maxwell relaxation time $\tau_{M1} = \tau_1$ decreases. This means that with increasing temperature, the degree of shielding of the external field increases due to the presence of a thin but powerful layer of bulk charge. An attention should be paid to the fact that the Maxwell relaxation time is a large value $\tau_{M1} = \tau_1 = 4.9 \cdot 10^{-3}$ s ($f_{\max 1} = 1/(2\pi\tau_1) = 32$ Hz for free electrons in AgJ at a temperature $T = 70°$C, i.e. significantly lower than the temperature $\gamma \to \beta$ PT (curves *1* in Fig. 1, 2)). At $T = 140–150°$C, i.e. in the region of $\beta \to \alpha$ AF, the Maxwell time in a narrow temperature range decreases by orders of magnitude from $\tau_{M1} = \tau_1 = 1.6 \cdot 10^{-4}$ to $1.6 \cdot 10^{-7}$ s ($f_{\max 1} = 10^3$ or 10^6 Hz — see curves *3, 4* in Fig. 1, 2), respectively. In other words, the electronic conductivity of the semiconductor layer increases by orders of magnitude.

The above allows proposing the following simple equivalent scheme — the left part of Fig. 6. C_sI — capacitance

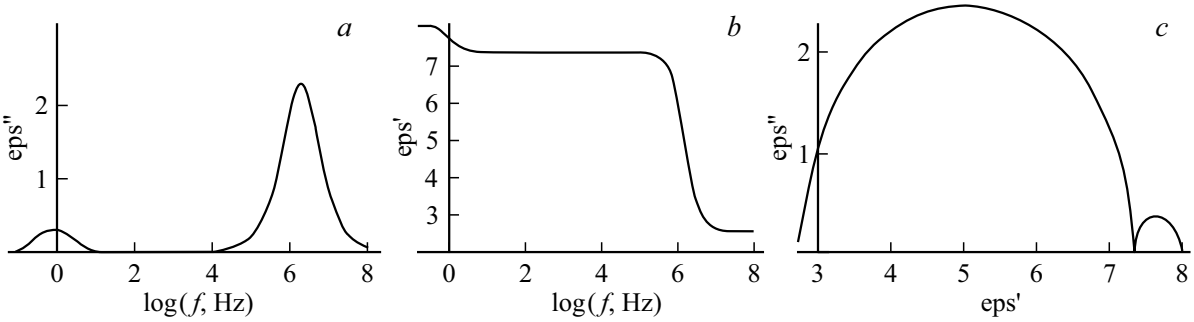

Figure 7. Frequency dependences calculated for the scheme Fig. 6 (a) imaginary ε'' and (b) valid ε' parts of the dielectric constant, (c) CC diagram — dependence $\varepsilon''(\varepsilon')$. $C_0 = 35$ pF, $C_sI = 245$ pF, $CI = 120$ pF, $RI = 400\,\Omega$, $C_sII = 35$ pF, $CII = 12$ pF, $RII = 3 \cdot 10^9\,\Omega$.

of the dielectric (mica) substrate, CI and RI — capacitance and ohmic resistance of the AgI semiconductor film at low temperatures $T < T_c$.

However, in the high temperature region, when $\beta \to \alpha$ the superionic semiconductor is perfect, i.e. at $T > T_c = 147°$C, in the low frequency region the value of ε changes quite sharply — an increase of $\varepsilon'(f \sim 0)$ and the step $\varepsilon'(f)$ is observed, as well as the second maximum of the function $\varepsilon''(f)$ and the second semicircle in the CC diagram — curves *8* Fig. 1, 2 and curve *4* Fig. 3. We associate such changes in the DS in the low-frequency region with additional shielding in the semiconductor film „of the residual" field in the spatial charge area. Such shielding is attributable to the „slow" drift of a large aggregate of positively charged silver ions. Additional shielding causes a decrease of the thickness of the spatial charge layer and contributes even more to the displacement of the electric field into the dielectric substrate. The dielectric permittivity of mica can be estimated from the radius of a small low-frequency semicircle in the CC diagram, equal to 0.25: $\varepsilon' = 8$ (it is worth reminding that $\varepsilon' = 2, 5$ occurs at $T < T_c$). The Maxwell relaxation time in the ion system Ag^+ is a very large value for free silver ions at $T = 250°$C, i.e. in the temperature range significantly exceeding the temperature of the superionic PT: $\tau_{M2} = \tau_2 = 1.6 \cdot 10^{-1}$ s ($f_{\max 2} = 1$ Hz, curves *8* in Fig. 1, 2). We emphasize that the maximum τ_{M2} of the function $\varepsilon'(f)$ manifests itself only at $T > T_c$ of the superionic PT (Fig. 1, 2).

A significant difference in the values of the times τ_{M1} and τ_{M2} ($\tau_{M1} \ll \tau_{M2}$) is due to the nature of the electrical conductivity of the AgI film. The mobility of free electrons is several orders of magnitude higher than the mobility of almost free, but massive, silver ions if the values of charges and concentrations of positive and negative charge carriers in the first approximation after $\beta \to \alpha$ PT coincide with each other at the same temperature (assuming a negligible concentration of electrons up to $\beta \to \alpha$ PT). Assuming that the mobility of μ microparticles in the first approximation is inversely proportional to their mass and comparing the masses of the ion Ag^+ and the electron, the value $\tau_{M1}/\tau_{N2} \sim 10^5$ is obtained, which, taking into account the expression $\tau_M = \varepsilon\varepsilon_0/(e^-)n\mu$, gives the value observed on 1) in the form of a difference of 5 orders of magnitude between the frequencies of the maxima position $f_{\max}$ of the function $\varepsilon'(f)$ for electrons and ions Ag^+ ($\tau_M = 1/2\pi f_{\max}$). Additional DS changes that occur after the PT is committed to the superionic phase can be described using an equivalent scheme (Fig. 6), complicated by the second circuit. RII represents the low-frequency ohmic resistance of a semiconductor along channels through which silver ions drift at high temperatures ($T > T_c$) of a superionic PT. CII — this is the capacity of a narrow layer of positive charge that arises as a result of electron drift and which further narrows as an additional positive charge of silver ions appears in it. CII — this is a part of the capacitance of the dielectric substrate, which is in total adjacent to the total set of conducting channels in AgJ nanocrystallites. Fig. 7 shows, as indicated, the calculation results performed in accordance with the equivalent scheme shown in Fig. 6. As we can see there is a good qualitative agreement between the experimental data and the calculation results. Quantitative characteristics of physical parameters are given in the figure caption.

Despite the good qualitative agreement, a careful detailed comparison shows that the maxima and steps on the experimental curves are somewhat wider than on the calculated curves, and the measured CC diagrams do not have the form of regular semicircles: „heights" semicircles of experimental CC diagrams are less than half of their „half-widths". The discrepancy established by careful comparison between experimental and calculated data is naturally explained, in our opinion, by the fact that the real sample contains a set of individual relaxers with relaxation times within each type of relaxers that are close, but do not coincide with each other, as predicted by Debye theory. That is, the discrepancy is, in our opinion, due to a certain distribution of the time density of relaxers over the numerical values of their times, which differs from the case of the delta function. In this more complex version of the model, different types of relaxers will appear in the form of a system of maxima of the function $\varepsilon''(f)$ and steps of the function $\varepsilon'(f)$ located closely in frequency, as well as several semicircles with similar characteristics on the KK diagram. At the same time, the presence of a set of separate relaxers with close relaxation times for each type of relaxers will manifest itself

in a distortion of the shape of the curves $\varepsilon'(f)$, $\varepsilon''(f)$ and the type of semicircles on the CC diagram.

The following possible reasons for the spread of numerical values of relaxation times can be named.

Since the experiments were carried out by us on thin-film nanocrystalline AgI samples having a strong spread across the diameters of the nanocrystallites composing the film [7], then individual nanocrystallites differ significantly in the radii r of the curvature of their surface. The energy of the surface tension of nanocrystallites, inversely proportional, according to Laplace's theorem, to the average radius of curvature of the crystal surface ($E_s \sim 1/r$), has a strong influence on the energy of phase transformations in single crystals, accompanied by a change in the symmetry of the lattice [8]. The mechanical stress caused by surface tension causes a change in the depth of the electron traps and, thereby, changes the mobility of electrons, affecting the conductivity of the material [9]. In addition, the mechanical stress also changes the value of the effective mass of the carriers [10], which again leads to a change in their mobility. An additional reason for the change in the conductivity of nanocrysallic films in relation to the conductivity of single crystals is that localized electronic states — near-surface electron traps [11] arise at the interfaces of nanocrystallites of the AgI film. The presence of near-surface traps leads to „sticking" on the surface of nanocrystallites of electrons freely moving in their volume with the formation of a surface electrostatic charge. This charge forms a strong ($\sim 10^5$ V/cm) electric field penetrating into the depth of the nanocrystallite and affecting the numerical value of the electrical conductivity. And, finally, it should be taken into account that silver halides are compounds of a transition element subject to strong electronic correlations [12], characterized by a significant dependence of the position of energy levels on their electron occupancy, which also makes adjustments to the numerical value of carrier mobility.

The relaxation time τ_1 in the model proposed in this paper is the Maxwellian relaxation time in a system of free conduction electrons. It is given by the expression $\tau_M = \varepsilon\varepsilon_0/\sigma$, where $\sigma = (e^-)n\mu$ is the specific electrical conductivity of the material. Therefore, all of these reasons can affect the spread of numerical values of relaxation times and, thereby, cause distortions of the characteristics of the DS in relation to the ideal case of the distribution of relaxers in the form of a delta function.

6. Conclusion

Summarizing, it can be stated that the shift of DS features observed in this work towards high frequencies with increasing temperature is explained by an increase in the rate of thermal generation of free electrons and, as a consequence, an increase in the electrical conductivity of the semiconductor, accompanied by a decrease in the Maxwell relaxation time. In addition, the formation of a superionic PT at a temperature of $T > T_c$ leads to the appearance of a „liquid" fraction of ions Ag^+ in nanocrystallites of the AgI film, as a result of which the electrical conductivity, in addition to the electronic, additionally acquires an ionic character. We would like to emphasize that the „liquid" ion fraction Ag^+ does not include the entire sublattice of silver ions, but occupies a relatively small fraction of the crystal in the form of ion-conducting channels between crystalline polytypes [13]. At the same time, the low mobility of silver ions causes a low ionic conductivity of the substance, a long Maxwell relaxation time for the ion array, and the appearance of a second feature in the DS at low frequencies corresponding to a long time τ_{M2}. This result clearly demonstrates the fact that the DS method allows, unlike other research methods, to study (separate) the electronic and ionic processes occurring in superionic PT separately.

Conflict of interest

The authors declare that they have no conflict of interest.

References

[1] T.Yu. Vergent'ev, E.Yu. Koroleva, D.A. Kurdyukov, A.A. Naberezhnova, A.V. Filimonov. Phys. Solid State **55**, *1*, 175 (2013).
[2] Fizicheskaya entsiklopediya. Sov. entsiklopediya, M. **1**, 700 (1988). (in Russian).
[3] Kittel. Introduction to solid state physics. John Wiley & Sons, Inc. John Wiley & Sons (2005). 680 p. ISBN 0-471-41526-X.
[4] A.V. Ilinskiy, R.A. Kastro, M.E. Pashkevich, E.B. Shadrin. FTP **54**, *4*, 331 (2020). (in Russian).
[5] D.N. Zubarev. Fizicheskaya entsiklopediya / Ed. by A.M. Prokhorov. Bol'shaya ros. enciklopediya, M. (1992). Ch. 5. (in Russian).
[6] I.O. Popova, N.Y. Gunia. Izv. RGPU im. A.I. Gercena, **144**, 51 (2012). (in Russian).
[7] E.S. Bochkareva, A.I. Sidorov, A.V. Nashchekin. ZhTF **7**, 1067 (2018). (in Russian).
[8] E.B. Shadrin, A.V. Ilyinsky, A.I. Sidorov, S.D. Khanin. FTT **44**, *11*, 2269 (2010). (in Russian).
[9] A.I. Slutsker, V.L. Gilyarov, Yu.I. Polikarpov. ZhTF **78**, *11*, 60 (2008). (in Russian).
[10] G.I. Zebrev. Fizicheskiye osnovy kremniyevoy nanoelektroniki. BINOM. Laboratoriya znanij, M. (2011). 240 p. ISBN 978-5-9963-0181-2 (in Russian).
[11] B.I. Bednyi. Elektronnye lovushki na poverhnosti poluprovodnikov. Sorosov. obraz. zhurn. Fizika **7**, 114 (1998). (in Russian).
[12] V.F. Gantmacher. Elektrony v neuporyadochennykh sredakh. FIZMATLIT, M. (2013). 288 p. (in Russian).
[13] R.V. Marija, S.V. Dragan, G.M. Vesna, J. Serb. Chem. Soc. **72**, *8–9*, 857 (2007).

Translated by A.Akhtyamov